ChemComm

COMMUNICATION

View Article Online
View Journal | View Issue

Cite this: *Chem. Commun.*, 2016, 52, 1254

Received 28th October 2015,
Accepted 18th November 2015

DOI: 10.1039/c5cc08884d

www.rsc.org/chemcomm

Switching first contact: photocontrol of *E. coli* adhesion to human cells†

L. Möckl,‡[a] A. Müller,‡[b] C. Bräuchle*[a] and T. K. Lindhorst*[b]

We have shown previously that carbohydrate-specific bacterial adhesion to a non-physiological surface can be photocontrolled by reversible *E*/*Z* isomerisation using azobenzene-functionalised sugars. Here, this approach is applied to the surface of human cells. We show not only that bacterial adhesion to the azobenzene glycoside-modified cell surface is higher in the *E* than in the *Z* state, but add data about the specific modulation of the effect.

Cell adhesion is a fundamental principle of biology. Many of its aspects have been elucidated,[1,2] but the molecular details of cell interactions are not fully understood. As the first contact of cells is mediated through their glycosylated surfaces, our research on cell adhesion is focused on carbohydrate recognition.

All organisms can recognise and distinguish between carbohydrates with the help of specialised proteins, the lectins.[3] Lectin function has been described in the context of, *i.e.*, signalling, trafficking, and quality control, thus involving indispensable processes of life.[4,5] Also bacterial cells utilise their own lectins to mediate adhesion to glycosylated surfaces such as the membrane of the target cells.[6,7] Furthermore, bacterial adhesion enables bacterial colonization, biofilm formation, biofouling, or it precedes infection of cells.[8,9] Hence, investigation and control of bacterial adhesion is important, especially in a medical context, given the high incidence rates of infectious diseases worldwide.[10]

In recent years we have studied the α-D-mannoside-specific adhesion of *Escherichia coli* bacteria,[11,12] which is mediated by the bacterial lectin FimH. FimH is located at the tips of adhesive organelles, called type 1 fimbriae,[13] which are projecting from the bacterial cell surface. Previously we have shown that type 1 fimbriae-mediated bacterial adhesion to a non-physiological surface can be photochemically controlled. In this specific case azobenzene-functionalised α-D-mannoside derivatives were assembled on a gold surface in the form of a glyco-SAM (self-assembled monolayer).[14,15] Photochemical isomerisation of the azobenzene moiety between its *E* and *Z* form then allowed to reversibly switch the orientation of the attached carbohydrate ligands. In parallel with this *E*/*Z* isomerisation, the adhesiveness of the surface was altered leading to reduction of bacterial adhesion in the *Z* state of the SAM by ~80% in comparison to the *E* state.

While the azobenzene photoswitch is long known[16] and has been used before for switching of the properties of designer surfaces,[17–20] our work on the control of bacterial adhesion through re-orientation of carbohydrate presentation is unprecedented. Here it has been our goal to challenge our system in the context of cell–cell adhesion, thus changing the artificial glyco-SAM surface against the plasma membrane of human cells. For this, we had to incorporate azobenzene mannosides in the cell surface of live cells, effect their *E*/*Z* isomerisation to switch the orientation of the attached mannoside moieties, and to finally test the influence of this isomerisation on *E. coli* adhesion.

Our experimental approach is explained in Fig. 1: metabolic oligosaccharide engineering (MOE)[21,22] was employed to install bioorthogonal azido groups on the cell surface. This allows their subsequent modification with alkyne-functionalised azobenzene glycosides by well-known click chemistry.[23–26] In a final step, photochemical *E*/*Z* isomerisation of the installed azobenzene moieties was effected by irradiation with light of the appropriate wavelength, and subsequently bacterial adhesion was measured *via* high-resolution live-cell fluorescence microscopy. For these experiments, human microvascular endothelial cells, variant 1 (HMEC-1) and GFP-fluorescent type 1 fimbriated *E. coli* PKL1162[27] were used.

To install the required bioorthogonal azido functional groups on the cell surface, HMEC-1 were incubated with 50 μM tetra-acetylated *N*-azidoacetyl-D-mannosamine (Ac_4ManNAz, Fig. 1). Ac_4ManNAz is taken up by the cells and proceeded to result in azido labelling of terminal sialic acid units of membrane glycoproteins. When Ac_4GalNAz is employed on the other hand, the

[a] *Department of Physical Chemistry, Ludwig Maximilian University of Munich, Butenandtstr. 11, D-81377 Munich, Germany*
[b] *Otto Diels Institute of Organic Chemistry, Christiana Albertina University of Kiel, Otto-Hahn-Platz 3/4, D-24118 Kiel, Germany. E-mail: tklind@oc.uni-kiel.de; Fax: +49 431-8807410*

† Electronic supplementary information (ESI) available: Synthetic procedures and analytical data of synthesised compounds, their photochromic properties, and fluorescence images. See DOI: 10.1039/c5cc08884d

‡ These authors contributed equally to the paper.

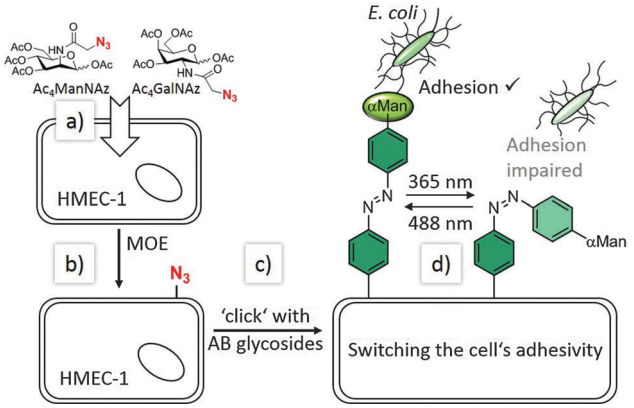

Fig. 1 Our approach of switching the adhesivity of cells. Azido groups can be incorporated into cell surface glycoconjugates according to metabolic oligosaccharide engineering (MOE): (a) synthetic carbohydrates (Ac_4ManNAz or Ac_4GalNAz) are taken up by the cells (HMEC-1) and processed by their biosynthetic machinery (b). Bioorthogonal click chemistry (c) then allows conjugation with azobenzene (AB) glycosides (such as AB α-D-mannosides, αMan) at the cell surface. Reversible *E*/*Z* isomerisation (d) employing UV or visible light, respectively, allows to change the orientation of the azobenzene-conjugated sugar and to manipulate sugar-specific bacterial adhesion in parallel.

azido label is incorporated into mucin-type glycoproteins.[28] For the chemical functionalisation of the azido-modified cells, the azobenzene derivatives **5–7**, carrying an alkyne functional group were required (Scheme 1). Synthesis started with the known *p*-aminophenyl glycosides **1**[27] and **2**,[29] which were subjected to a classical azo coupling with phenol to furnish the respective hydroxyazobenzene derivatives **3** and **4**.[30] Then, Williamson etherification with propargyl bromide led to the desired alkyne-functionalised azobenzene glycosides **5** and **6**. The azobenzene alkyne **7** was needed as control and was directly obtained from hydroxyazobenzene.[31]

At first, the azobenzene α-D-mannoside **5** was conjugated to azido-functionalised HMEC-1 after Ac_4ManNAz labelling. For this reaction, 200 μM azobenzene α-D-mannoside, 50 μM $CuSO_4$, 250 μM tris(3-hydroxypropyltriazolylmethyl)amine, 1 mM aminoguanidine, and 2.5 mM sodium ascorbate in buffered saline solution were employed at 4 °C for 5 minutes.[32] A 200 μM solution of **5** was sufficient to ensure complete labelling of all azido groups on the cell surface (*cf.* ESI,† Fig. S13). Copper(I), which is produced during the reaction, is known to exhibit toxic side effects after some time, however, we applied conditions that were shown earlier not to be harmful for cells.

Labelled cells were split into two portions and both sets were irradiated with UV light (365 nm), to effect $E \rightarrow Z$ isomerisation of the conjugated azobenzene moiety. Then, cells were incubated with GFP-fluorescent *E. coli* (*cf.* ESI,† Fig. S14–S18) and the number of adhered bacteria was counted employing high-resolution live-cell fluorescence microscopy. For both sets of HMEC-1 the number of adhered bacteria is similarly low at this stage, as it is expected (Fig. 2).

In a subsequent step, only one of both cell sets was irradiated again; this time with green light (488 nm) to reverse the initial isomerisation and thus effect $Z \rightarrow E$ isomerisation of the azobenzene configuration. Then, a second incubation with fluorescent *E. coli* was performed, and adhesion again quantified. Whereas the adhesivity of the cells without a second irradiation treatment remained the same, a significant increase of bacterial adhesion was measured for the cells that were irradiated at 488 nm (about 50%). We attribute this observation to the mode of mannose orientation, which is changed with the isomerisation of the azobenzene hinge. In accordance with the observation made with photoswitchable glyco-SAMs,[15] the adhesivity of the azobenzene mannoside-modified cell surface is higher in the *E* than in the *Z* state.

In order to investigate photoswitching of cell adhesion in real-time, flow-based experiments[33] were performed next. Thus, HMEC-1 were cultivated in flow chambers, again incubated with Ac_4ManNAz and labelled with azobenzene mannoside **5** in analogy to our experiments under static conditions. Then, a bacterial suspension (1 : 50 dilution of a suspension with OD_{600} = 0.1) was employed at continuous flow with a shear rate of 1.5 dyn cm^{-2} (a typical shear rate for microvascules). The flow was not interrupted during irradiation (300 seconds). Adhering bacteria were monitored by fluorescence microscopy while switching the configuration of HMEC-conjugated azobenzene mannosides multiple times between

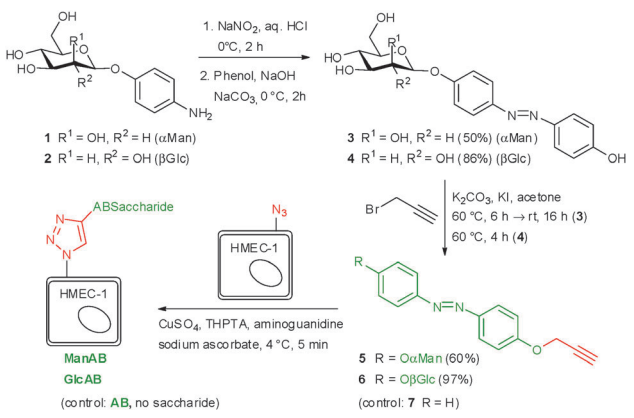

Scheme 1 Synthesis of alkyne-functionalised azobenzene glycosides and labelling of engineered human cells (HMEC-1). The α-D-mannopyranoside **5** was used as specific ligand for bacterial adhesion and the β-D-glucopyranoside **6** and **7** were needed as control compounds.

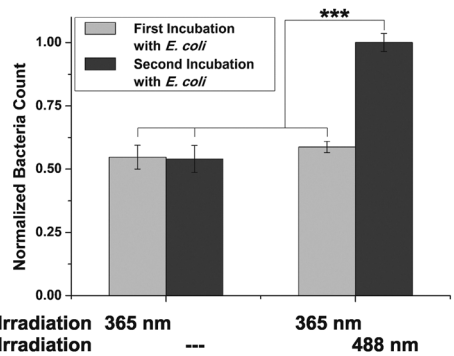

Fig. 2 Switching of **ManAB** configuration allows to control adhesion of *E. coli*. After incubation of two sets of Ac_4ManNAz-engineered HMEC-1, conjugated with **5** in *Z*-configuration, bacterial adhesion is similar for both sets. Switching of **ManAB** configuration to *E* (365 nm) increases bacterial adhesion (second incubation). Error bars are standard error of the mean (SEM) of experiments with four independent sets of cells/condition. ***$p < 0.001$ (*cf.* ESI,† Fig. S14).

E and *Z* (Fig. 3). The development of the recorded bacterial GFP-fluorescence is then a direct measure for the adhesion of *E. coli*. The obtained curves clearly show that alternating irradiation using light of 365 nm and 488 nm has a strong effect on bacterial adhesion (Fig. 3a). After irradiation of the flow chamber with 488 nm light, the slopes of the bacterial GFP signal are significantly higher than after irradiation with 365 nm. This is also clearly seen after fitting of the curves, assuming a linear development of fluorescence (Fig. 3b).

Only after several switching events (starting at 1500 s), the measured slopes are no longer correlated with azobenzene configuration. This can be attributed to increasing coverage of HMEC-1 with bacterial cells (see also microscopic images, ESI,† Fig. S19). When more and more bacteria adhere to bacterial cells and not to HMEC-1, the adhesion is naturally not sensitive to *E*/*Z* isomerisation.

As under static conditions, the results obtained in the flow experiments indicate that the orientation of mannoside **5** conjugated to the surface of HMEC-1 has a strong influence on the adhesion of bacteria, suggesting that the bent *Z* form is less accessible for bacteria than the *E* form. Thus, adhesion is reduced after $E \rightarrow Z$ isomerisation. Next, two important control experiments were performed in order to understand the observed effects in greater detail. First, the question of carbohydrate specificity of the observed effects was addressed by employing the azobenzene derivative **7** (**AB** in Fig. 4) devoid of a carbohydrate, and the β-D-glucoside **6** (**GlcAB** in Fig. 4) for HMEC-1 labelling. The glucoside **6** exhibits a similar structure and polarity as **5** but is no ligand for the bacterial lectin FimH. Labelling of HMEC-1 was done as before and bacterial adhesion measured after irradiation. All experiments were compared to azido-labelled HMEC-1, which had not been reacted with either of the azobenzene derivatives (Control in Fig. 4).

These experiments show that adhesion of *E. coli* to cells reacted with either **6** or **7**, is significantly decreased compared to untreated cells. This observation suggests a shielding effect for both derivatives, prohibiting bacterial adhesion to the surface of HMEC-1 to some extent. On the other hand, this effect is not significantly sensitive to *E*/*Z* isomerisation. This finding indicates that the adhesion of bacteria to cells treated with **5** is indeed carbohydrate-specific. Control cells showed a slight response to irradiation with 365 nm light, but the effects caused by **6** or **7** are more significant.

How can the orientation of a rather small molecule (such as an azobenzene glycoside) within the complex environment of a cell's surface exert such a pronounced effect on cell adhesion? To answer this question, the azobenzene mannoside ligand was positioned differently on the surface of HMEC-1. This is possible by labelling HMEC-1 with Ac_4GalNAz instead of Ac_4ManNAz. Whereas Ac_4ManNAz leads to labelling of sialic acids, which are almost exclusively found at the terminal positions of cell surface glycans, Ac_4GalNAz labels mucin-type glycoproteins. These are characterised by LacNAc moieties, which are localised deeper within the glycosylated cell surface.[28]

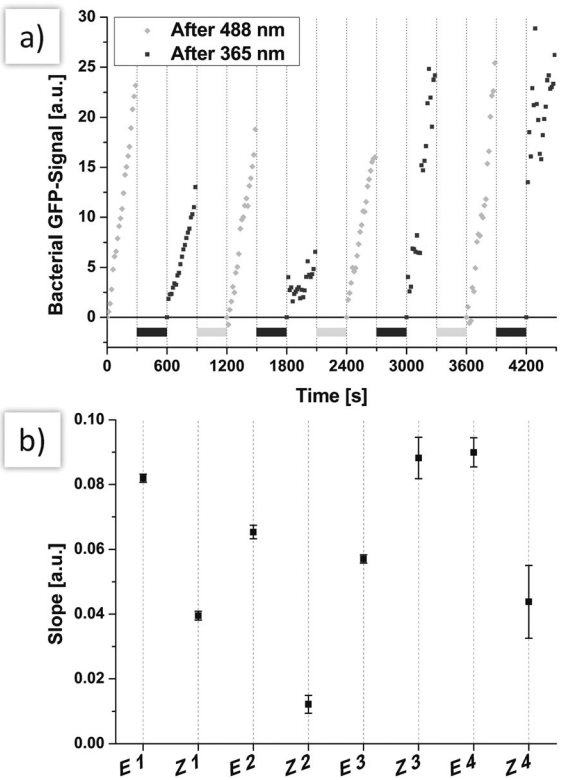

Fig. 3 (a) The azobenzene mannoside **5** was switched several times between *Z* and *E* while flowing a continuous stream of bacterial solution over the cells. The adhesion of bacteria was lower if **5** was in *Z*-configuration. Only after several switching cycles this tendency was no longer observed, caused by increasing coverage of the cells with bacteria. During irradiation with 365 nm (light grey bars) or 488 nm (dark grey bars), the flow was not stopped. (b) The slopes of linear curves that were fitted to the data of the middle panel clearly resembles the effect of reversible switching. Error bars are given as SEM of the fitting. For easier comparison, the slopes are set to start at a common origin by subtraction of the fluorescence intensity of the first frame from the subsequent frames.

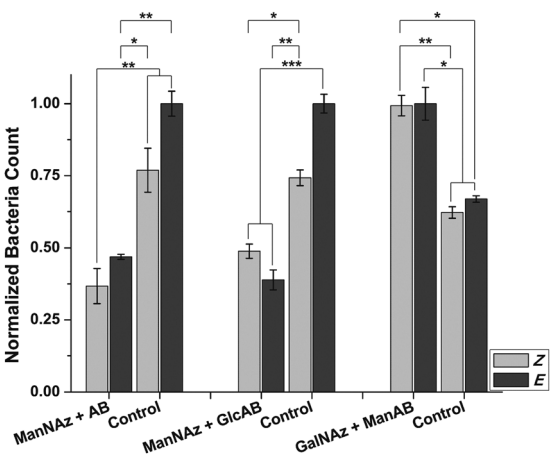

Fig. 4 Control experiments. Left & middle: Ac_4ManNAz labelling and conjugation with **AB** (no sugar residue) or **GlcAB** (β-Glc instead of α-Man) leads to reduced adhesion in comparison to control cells independent of **AB** configuration. Right: Ac_4GalNAz labelling and conjugation with **ManAB** leads to increased adhesion independent of AB configuration. Errors are given as SEM. Four independent sets of cells were tested for each condition. $*p < 0.1$, $**p < 0.01$, $***p < 0.001$.

Indeed, bacterial adhesion to HMEC-1, labelled with Ac_4GalNAz and modified with mannoside **5** is increased in comparison to control cells (Fig. 4). This observation can be rationalised by the increased concentration of mannosides present on the cell surface after modification. However, the observed increased adhesion is not photosensitive in this case. As LacNAc groups are typically not exposed at the cell surface, conjugated **ManAB** moieties might be buried under a layer of other glycoconjugates so that an orientational change of mannoside ligands is not effective. On the other hand, we cannot measure the extent of azobenzene isomerisation, which might be different in both investigated cases (Ac_4ManNAz or Ac_4GalNAz labelling).

Taken together, we show that the azobenzene mannoside **5** can be employed to influence adhesion of *E. coli* to HMEC-1. We postulate the following mechanism that underlies this photocontrol: (i) bacterial FimH binds to mannose, which serves as ligand for specific interaction between the bacterium and the modified cell surface (*cf.* Ac_4ManNAz + **5** *vs.* Ac_4ManNAz + **6**). (ii) If no mannose ligand is present or if it adopts a disadvantageous orientation (*Z*-configuration), the azobenzene groups shield the cell, leading to reduced binding of *E. coli* (*cf.* Ac_4ManNAz + **5** *vs.* Ac_4ManNAz + **AB**). (iii) The FimH ligand mannose must be localised at the terminus of glycans to ensure that the change in configuration upon a *Z*/*E* transition is not small (Ac_4ManNAz + **5** *vs.* Ac_4GalNAz + **5**).

It is surprising that this orientation effect can be found not only on an artificial, ordered glyco-SAM as we described before,[15] but even in the complex, in comparison rather chaotic setting of the cell surface. Of course, this finding bears implications for the way how cells interact with their environment and offers options for prevention of bacterial adhesion with temporal and spatial resolution.

Financial support by SFB 677 is gratefully acknowledged. We also thank the excellence clusters Nano Systems Initiative Munich (NIM), the Centre for Integrated Protein Science Munich (CIPSM), and the Centre for Nanoscience Munich (CeNS).

Notes and references

1 A. A. Khalili and M. R. Ahmad, *Int. J. Mol. Sci.*, 2015, **16**, 18149–18184.
2 M. E. Taylor and K. Drickamer, *Curr. Opin. Cell Biol.*, 2007, **19**, 572–5772.
3 N. Sharon and H. Lis, *Glycobiology*, 2004, **14**, 53R–62R.
4 C. R. Bertozzi and L. L. Kiessling, *Science*, 2001, **291**, 2357–2364.
5 F.-T. Liu and G. A. Rabinovich, *Nat. Rev.*, 2005, **5**, 29–41.
6 I. Ofek, D. Mirelman and N. Sharon, *Nature*, 1977, **265**, 623–625.
7 K. Ohlsen, T. A. Oelschlaeger, J. Hacker and A. S. Khan, *Top. Curr. Chem.*, 2009, **288**, 17–65.
8 L. Hall-Stoodley, J. W. Costerton and P. Stoodley, *Nat. Rev. Microbiol.*, 2004, **2**, 95–108.
9 D. Ribet and P. Cossart, *Microbes Infect.*, 2015, **17**, 173–183.
10 K. E. Jones, N. G. Patel, M. A. Levy, A. Storeygard, D. Balk, J. L. Gittleman and P. Daszak, *Nature*, 2008, **451**, 990–993.
11 M. Hartmann and T. K. Lindhorst, *Eur. J. Org. Chem.*, 2011, 3583–3609.
12 A. Bernardi, *et al.*, *Chem. Soc. Rev.*, 2013, **42**, 4709–4727.
13 J. Lillington, S. Geibel and G. Waksman, *Biochim. Biophys. Acta*, 2014, **1840**, 2783–2793.
14 V. Chandrasekaran, H. Jacob, F. Petersen, K. Kathirvel, F. Tuczek and T. K. Lindhorst, *Chem. – Eur. J.*, 2014, **20**, 8744–8752.
15 T. Weber, V. Chandrasekaran, I. Stamer, M. B. Thygesen, A. Terfort and T. K. Lindhorst, *Angew. Chem.*, 2014, **126**, 14812–14815 (*Angew. Chem., Int. Ed.*, 2014, **53**, 14583–14586).
16 G. S. Hartley, *Nature*, 1937, **140**, 281.
17 J. Auernheimer, C. Dahmen, U. Hersel, A. Bausch and H. Kessler, *J. Am. Chem. Soc.*, 2005, **127**, 16107–16110.
18 P. M. Mendes, *Chem. Soc. Rev.*, 2008, **37**, 2512–2529.
19 W. R. Browne and B. L. Feringa, *Annu. Rev. Phys. Chem.*, 2009, **60**, 407–428.
20 M.-M. Russew and S. Hecht, *Adv. Mater.*, 2010, **22**, 3348–3360.
21 E. M. Sletten and C. R. Bertozzi, *Acc. Chem. Res.*, 2011, **44**, 666–676.
22 M. S. Siegrist, B. M. Swarts, D. M. Fox, S. A. Lim and C. R. Bertozzi, *FEMS Microbiol. Rev.*, 2015, **39**, 184–202.
23 V. V. Rostovtsev, L. G. Green, V. V. Fokin and K. B. Sharpless, *Angew. Chem.*, 2002, **114**, 2708–2711 (*Angew. Chem., Int. Ed.*, 2002, **41**, 2596–2599).
24 M. Meldal and C. W. Tornøe, *Chem. Rev.*, 2008, **108**, 2952–3015.
25 M. Kleinert, T. Winkler, A. Terfort and T. K. Lindhorst, *Org. Biomol. Chem.*, 2008, **6**, 2118–2132.
26 C. Grabosch, M. Kind, Y. Gies, F. Schweighöfer, A. Terfort and T. K. Lindhorst, *Org. Biomol. Chem.*, 2013, **11**, 4006–4015.
27 M. Hartmann, A. K. Horst, P. Klemm and T. K. Lindhorst, *Chem. Commun.*, 2010, **46**, 330–332.
28 J. M. Baskin, J. A. Prescher, S. T. Laughlin, N. J. Agard, P. V. Chang, I. A. Miller, A. Lo, J. A. Codelli and C. R. Bertozzi, *Proc. Natl. Acad. Sci. U. S. A.*, 2007, **104**, 16793–16797.
29 G. R. Gustafson, C. M. Baldino, M.-M. E. O'Donnell, A. Sheldon, R. J. Tarsa, C. J. Verni and D. L. Coffen, *Tetrahedron*, 1998, **54**, 4051–4065.
30 V. Chandrasekaran, E. Johannes, H. Kobarg, F. D. Sönnichsen and T. K. Lindhorst, *ChemistryOpen*, 2014, **3**, 99–108.
31 G. Mantovani, V. Ladmiral, L. Tao and D. M. Haddleton, *Chem. Commun.*, 2005, 2089–2091.
32 V. Hong, N. F. Steinmetz, M. Manchester and M. G. Finn, *Bioconjugate Chem.*, 2010, **21**, 1912–1916.
33 E. V. Sokurenko, V. Vogel and W. E. Thomas, *Cell Host Microbe*, 2008, **4**, 314–323.